



Nintedanib effects on delaying cancer progression and decreasing COX-2 and IL-17 in the prostate anterior lobe in TRAMP mice

Letícia Ferreira Alves, Raquel Frenedoso da Silva, Valéria Helena Alves Cagnon*

Department of Structural and Functional Biology, Institute of Biology, University of Campinas (UNICAMP), São Paulo, Brazil

ARTICLE INFO

Keywords:

Prostate cancer
Nintedanib
Inflammation
TRAMP
IL-17
COX-2

ABSTRACT

Prostate cancer is the most prevalent type of cancer in men around the world. Due to its high incidence, new therapies have been evaluated, including drugs capable of inhibiting the FGF/VEGF pathways, as Nintedanib. The aim herein was to evaluate the Nintedanib therapeutic effects on morphology and COX-2 and IL-17 levels in the prostate anterior lobe in different grades of the tumor progression in TRAMP mice. Animals were treated with Nintedanib at a dose of 10 mg/kg/day in initial and intermediate grades of tumor development. At the end of treatment, the prostate anterior lobe was collected and submitted to morphological, immunohistochemical and Western Blotting analyses. The results showed that Nintedanib delayed the prostate carcinogenesis progression, with over 20% of reduction in frequency of tissue injuries, particularly in the group treated from 12 to 16 weeks of age. Also, decreased COX-2 and IL-17 levels were observed in both groups treated with Nintedanib in the prostate anterior lobe. Thus, we concluded that Nintedanib was effective in delaying tumor progression and, despite not directly acting on inflammation, Nintedanib may adversely affect inflammatory pathways, favoring prostate cancer delay.

1. Introduction

The prostate cancer is among the four major cancer incidence in the world and it is estimated that one in every seven men in the US will be diagnosed with this malignancy in their lifetime (Siegel et al., 2016). It is known that epithelial-stromal interactions are essential for the maintenance of prostate homeostasis in adults and hormonal imbalance and/or setup of inflammatory processes are directly related to prostate carcinogenesis (Barron and Rowley, 2012). Prostatic adenocarcinoma begins with precancerous lesions known as prostatic intraepithelial neoplasia (PIN) (De Marzo et al., 2003). These lesions are characterized by loss of cell polarity, nuclear atypia, and focal dysplasia which results in cell invasion in the lumen of prostatic ducts (Zynger and Yang, 2009). PIN to carcinoma progression involves the basal lamina disruption and proliferation of tumor cells through the prostatic stroma (Tuxhorn et al., 2001). Different biological processes are involved in prostate cancer development such as inflammation that is responsible for over 20% of cancer setups (Sfanos and de Marzo, 2012). The inflammatory response in the prostate generally results in changes in the glandular microenvironment, such as intense stromal remodeling, fibroblast activation, immune cells infiltration and collagen accumulation (Mimeault and Batra, 2013).

Different drugs have been evaluated for cancer treatment, including Nintedanib (BIBF-1120), a derivative of indolinone molecule, acting as selective angioquinases inhibitor, since the drug acts on FGFR, PDGFR, and VEGFR pathways, preventing proliferation of the cell types expressing them. Nintedanib also acts by inhibiting cell proliferation and apoptosis in three cell types involved in angiogenesis: endothelial cells, pericytes and smooth muscle cells (Hilberg et al., 2008). In addition to its anti-angiogenic activity, Nintedanib has shown anti-inflammatory properties in idiopathic pulmonary fibrosis, leading to a reduction of inflammatory cells such as lymphocytes and neutrophils in the lung tissue, and a decrease in cytokine levels (Wollin et al., 2014). When administered for pancreatic cancer treatment, Nintedanib caused proliferation inhibition in multiple lineage cells, besides apoptosis induction and PI3K/MAPK activity blockage (Awasthi et al., 2015). Nintedanib use in human cancer cell culture showed significant results in cell growth inhibition as well as cell survival reduction. In vascular endothelial cells; pericytes and smooth muscle cell cultures, Nintedanib showed a potential to inhibit the pro-angiogenic signaling pathway and cell growth (Hilberg et al., 2008).

Thus, the aim herein was to evaluate the anti-tumor and anti-inflammatory capacity of Nintedanib by means of structural and molecular parameters in the anterior prostate lobe of TRAMP mice in

* Corresponding author at: Department of Structural and Functional Biology, Institute of Biology, State University of Campinas (UNICAMP), P.O. Box 6109, 13083-865, Campinas, São Paulo, Brazil.

E-mail address: quitete@unicamp.br (V.H.A. Cagnon).

<https://doi.org/10.1016/j.tice.2017.12.008>

Received 7 March 2017; Received in revised form 15 December 2017; Accepted 24 December 2017

Available online 27 December 2017

0040-8166/ © 2017 Elsevier Ltd. All rights reserved.

different periods of lesion development.

2. Material and methods

2.1. Animals and experimental procedures

A total of 25 male transgenic TRAMP mice (C57BL/6-Tg(TRAMP)8247Ng/JX FVB/Unib) F1/J were provided by the Multidisciplinary Center for Biological Investigation on Laboratory Animal Science (CEMIB) at the University of Campinas. All the mice received water and solid ration *ad libitum* (Nuvilab, Colombo, PR, Brazil) and were kept in the animal housing in the Department of Structural and Functional Biology, Institute of Biology. The TRAMP mice were separated into experimental groups; control groups (TC) and Nintedanib groups (TN) ($n = 5/\text{group}$). The control group was divided into TC8 (8 week old mice), TC12 (12 week old mice) and TC16 (16 week old mice), receiving the vehicle (Tween 20 (10%)) *via* gavage, five times a week for four weeks, whereas Nintedanib group was divided into TN12 (12 week old mice) and TN16 (16 week old mice), treated from 8 to 12 week and from 12 to 16 week of age (Fig. 1), respectively, with 10 mg/Kg/day dose, five times a week for four weeks (modified Hilberg et al., 2008; Bousquet et al., 2011; Silva et al., 2017).

At the end of the treatment, the mice were weighed on a Denver P-214 (Denver Instrument Company, Arvada, CO, EUA), anesthetized with 2% xylazine hydrochloride (5 mg/kg; König, São Paulo, Brazil) and 10% ketamine hydrochloride (60 mg/kg; Fort Dodge, Iowa, USA) and euthanized (Ethical approval: Committee for Ethics in Animal Research—University of Campinas, protocol n°: 4020-1). Samples from the anterior prostate lobe were collected for morphological, immunohistochemical and Western Blotting evaluations. The Western Blotting analyses were performed in the contralateral anterior prostate lobe from the same animal used to immunohistochemical/morphological evaluation.

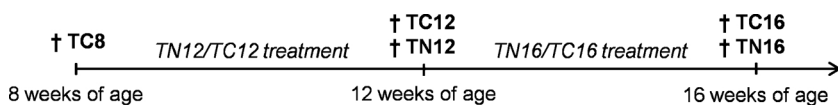
2.2. Morphological analysis

Samples from the anterior prostate lobe of TRAMP (Transgenic Adenocarcinoma of the Mouse Prostate) mice were collected from five animals per group and fixed in Bouin's solution for 24 h. Then, tissues were rinsed in 70% ethanol, dehydrated and embedded in plastic polymers (Paraplast, Sigma Aldrich, St Louis, MO, USA). The samples were cut in a Hyrax M60 microtome (Zeiss, Munich, Germany) and then stained with hematoxylin–eosin and Masson's Trichrome.

For characterization of the prostatic lesions, 15 random fields of tissue were photographed for each animal, totalizing 75 fields for experimental group. For morphological characterization, each photographed field were analyzed using a grid with 160 intersections (Weibel, 1963) and the epithelium conditions were diagnosed and recorded until reaching a total of 1000 points for each animal, totalizing 5000 points of prostatic epithelium analyzed per experimental group. Thus, all the experimental animals had the same amount of epithelium analyzed. The analyzed prostatic epithelium features were categorized between healthy epithelium (healthy feature) or injured, and the injuries were classified in low or high grade intraepithelial neoplasia and poorly differentiated adenocarcinoma (modified Berman-Booty et al., 2012; Kido et al., 2016).

2.3. Immunohistochemistry

The same processing protocol for morphological analyses was used



for samples submitted to immunohistochemistry. Antigen retrieval was performed by incubation of the cuts in citrate buffer (pH 6.0) at 100 °C for 10 min in microwave (750W power). Blockage of endogenous peroxidases was obtained with H₂O₂ (0.3% in methanol) for 20 min with subsequent incubation in blocking solution containing bovine serum albumin (3%) in TBS-T buffer for 1 h at room temperature. Subsequently, COX-2 and IL-17 antigens were immunolocalized using the antibodies: monoclonal mouse (sc-376 861) (Santa Cruz Biotecnology, USA) for COX-2 and polyclonal rabbit (sc-7927) (Santa Cruz Biotecnology, USA) for IL-17. Then, the sections were then washed with TBS-T and subsequently incubated in HRP-conjugated secondary antibody goat anti-rabbit IgG (W4018) (Promega Corporation, Madison, WI) for IL-17 and goat anti-mouse IgG (W4021) (Promega Corporation, Madison, WI) for COX-2. After washing in TBS-T, peroxidase activity was detected using a diaminobenzidine (DAB) chromogen (Sigma-Aldrich, St. Louis, MO) for 5 min, which indicated the immunoreactivity of antibodies. Harris hematoxylin was used for counter-staining. The slides were dehydrated, mounted and evaluated in the light microscope Nikon Eclipse E-400 (Nikon, Tokyo, Japan). Prostatic sections of each experimental animal were evaluated using the brown DAB precipitate – which indicates the immunoreactivity of antibodies – and analyzed using a multipoint system (Weibel, 1963) with 160 intersections. Fifteen random fields per animal were photographed and the percentage of immunoreactivity was evaluated by counting the coinciding brown areas with the grid intersection divided by the total number of points. The result was expressed as a relative frequency of positive staining for molecules in all experimental groups.

2.4. Western blotting

Prostate anterior lobe samples from four animals per group were collected and frozen in liquid nitrogen. The samples were weighed and homogenized in a Polytron homogenizer (Kinematica Inc., Lucerne, Switzerland) in a 40 mL/mg protein extraction buffer. The homogenized tissues were centrifuged at 14,000 rpm for 20 min at 4 °C and a sample of each extract was used for protein quantification with Bradford reagent (Bio-Rad Laboratories, Hercules, CA). The supernatants were mixed (1:1) with 3X Laemmli buffer and transferred to a dry bath at 100 °C for 5 min. Aliquots containing 75 mg of protein were separated by electrophoresis in SDS-PAGE gels under reducing conditions. After electrophoresis, proteins were transferred to Hybond-ECL nitrocellulose membranes (Amersham, Pharmacia Biotech, Arlington Heights, IL) at 120 V for 90 min. The membranes were blocked with BSA in TBS-T for 60 min and incubated at 4 °C overnight with the primary antibodies for COX-2, using monoclonal mouse anti-COX-2 (sc-376861) (Santa Cruz Biotechnology, USA). The membranes were then incubated for 2 h with the same HRP-conjugated secondary antibodies used for immunohistochemistry diluted in 1:6000 in 1% BSA. After washing in TBS-T, peroxidase activity was detected through the incubation of the membranes in the chemiluminescent solution (Pierce Biotechnology, Rockford, IL) for 5 min, followed by fluorescence capture using the Gene Gnome equipment and the Gene Sys image acquisition software (Syngene Bio Imaging, Cambridge, UK). Mouse monoclonal anti- β -actin (sc-81178) (Santa Cruz Biotechnology, CA) antibody was used as an endogen control for comparison among groups. The intensity of antigen bands in each experimental group was determined by densitometry using the Image J (Image Analysis and Processing in Java) software for image analyses and was expressed as the mean percentage in relation to β -Actin band intensity.

Fig. 1. Experimental groups. († = euthanized mice).

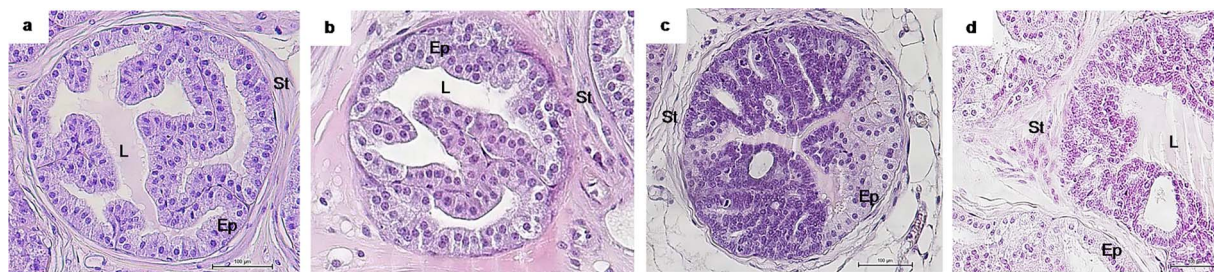


Fig. 2. Morphological parameters of the anterior lobe of the prostate A. Healthy prostate lobe (considered normal). B. Low grade PIN. C. High grade PIN D. Well-differentiated adenocarcinoma.

2.5. Statistical analysis

Data are presented as average percentage or mean ± Standard Error of Mean (SEM). Parametric variables were compared by ANOVA followed by the test of Turkey or by two-tailed *t*-test (for morphology and Western Blotting analysis). Differences were considered significant when $p < 0.05$. The statistical analyses were performed by the software GraphPad Prism (version 5.0).

3. Results

3.1. Morphological analysis

The prostate anterior lobe of TRAMP mice euthanized at 8 weeks of age (TC8) showed a high proportion of healthy epithelium (96.3%) (Fig. 4.A), characterized by a simple epithelium with columnar secretory cells with central nuclei, intermingled with basal cells (Fig. 2.A). Also, the prostatic acinar epithelium in the TC8 group showed 2.9% low-grade PIN (Figs. 3.A and 4.B), characterized by abnormal proliferation of acinar epithelial cells with cellular atypia such as nuclear size increase, cytoplasmic reduction and cell polarity loss without invasion of the glandular lumen (Fig. 2.B). The high grade PIN type of lesions was found in low frequency, accounting for only 0.8% of the total epithelium analyzed. The prostatic stroma in the TC8 group mostly presented, fibrillar element distribution around the glandular acini, without characterizing the collagen fiber layer thickening. In addition, there were smooth muscle cells and fibroblast without

abnormal features (.B).

The TC12 group animals showed a low percentage of healthy glandular epithelium, representing 85.1% (Figs. 3.A and 4.C). Glandular areas with low and high grade PIN represented 11.4 and 3.5%, respectively of the analyzed tissue (Figs. 3.B and C and 4.C). The high grade PIN was characterized by intense epithelial cell proliferation, presenting cribriform projections, breaking through the acinar lumen (Fig. 2.C).

The TC12 group presented glandular stroma with frequent collagen fiber layer thickening foci as well as an increased frequency of cellular elements, characterizing stromal hypertrophy (Fig. 4.D). On the other hand, the TN12 group showed more than 91.5% of uninjured glandular epithelium (Figs. 3.A and 4.E). The TN12 group also presented 5.5% of low grade PIN and 3.1% of high grade PIN, representing a reduction in the lesion area compared to the TC12 group (Figs. 3.B and C and 4.E). There was no well-differentiated adenocarcinoma in the TN12 group. The glandular stroma showed itself to be mostly healthy with occasional collagen fiber thickening areas (Fig. 4.F) in the TN12 group.

The control group with 16 week old mice (TC16) presented more than 40% injured epithelium, characterized by 24.6% of low grade PIN, 17% of high grade PIN and 0.3% of well-differentiated adenocarcinoma (Figs. 3.B and C and 4.G), with basal membrane disruption and occurrence of epithelial cells in the stroma (Fig. 2.D). The prostatic stroma in the TC16 animals showed a marked fibromuscular layer thickening, in addition to an apparent cell element frequency increase (Fig. 4.H). In contrast, the prostate from the TN16 group showed around 20% injured epithelium (Fig. 3.B and C), representing a significant decrease in

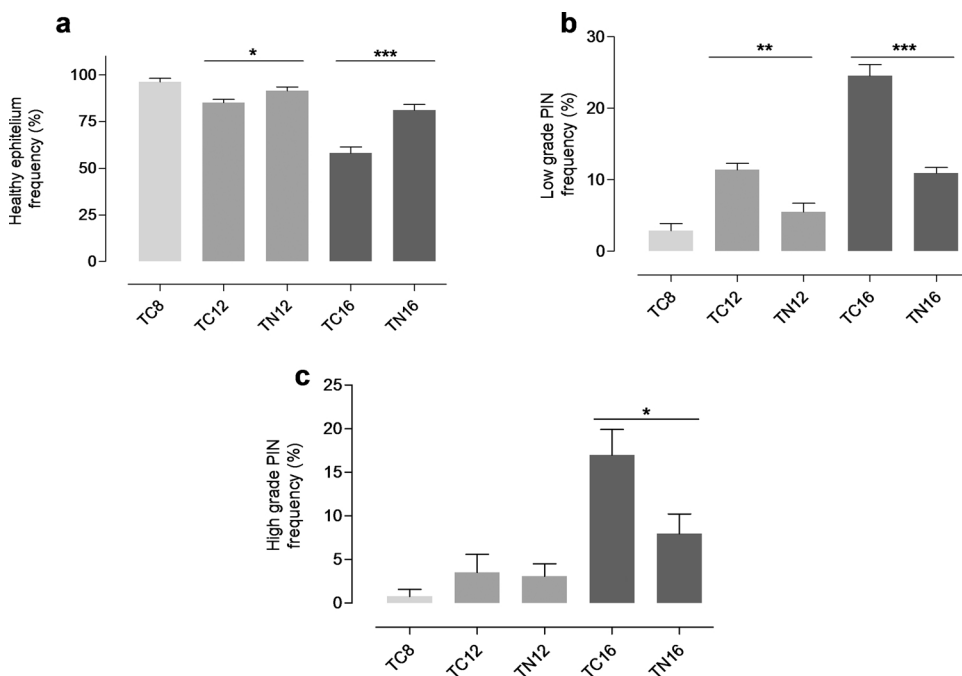


Fig. 3. Frequency (%) of healthy epithelium (A), low-grade PIN (B) and high-grade PIN (C) in the different experimental groups. * = $p < 0.05$, ** = $p < 0.01$, *** = $p < 0.001$.

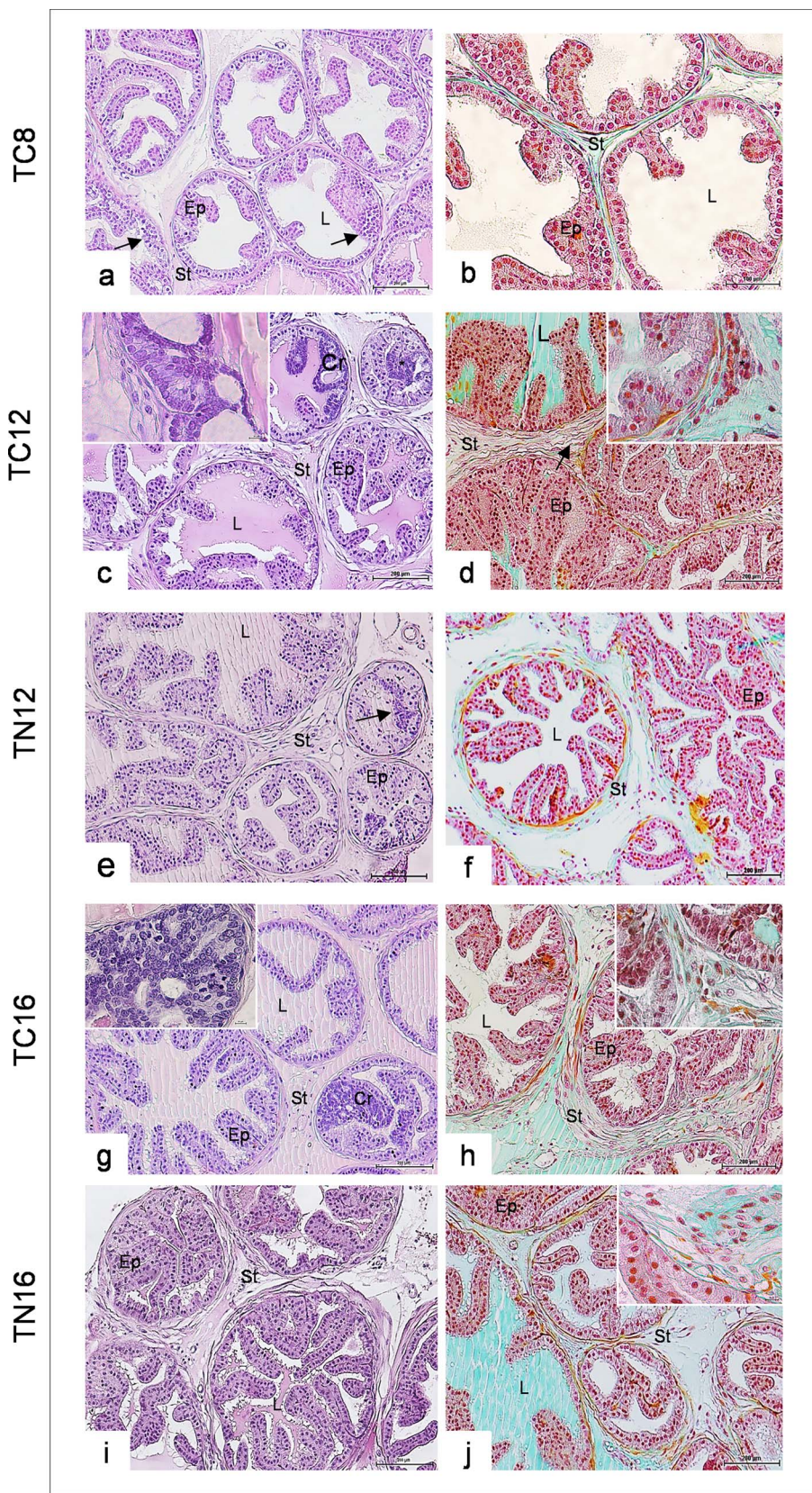


Fig. 4. Photomicrographs of the prostate anterior lobe A/ B. TC8 group – Epithelium and stroma showing healthy glandular tissue C. TC12 group – Acini presenting low-grade PIN (*) and high-grade PIN with cribriform features (Cr) D. TC12 group- Stroma presenting a thickening of the collagen fiber layer (arrow) and inflammatory cell accumulation (inset/*) E. TN12 group – Healthy epithelium and some low-grade PIN occurrence (arrow) F. TN12 group – Stromal fibrillar elements with a regular distribution around the acini G. TC16 group- Acini presenting high-grade PIN with cribriform features (Cr) (Inset) H. TC16 group – Hypertrophied fibromuscular layer. Atrophy of epithelial cells and thickened collagen fibers (inset) I. TN16 group – Healthy epithelium J. TN16 group – Slight thickening of the collagen fibers layer. Ep = epithelium; St = stroma; L = lumen; Cr = cribriform. H &E on the left and Masson's Trichrome on the right.

comparison to the TC16 group. The TN16 group presented 10.9% of low grade PIN and 7.9% of high grade PIN (Figs. 3.B and C and 4.I). The treated group (TN16) presented acini surrounded by thin fibromuscular layers, characterizing a non-hypertrophic stroma; also, stromal hyperplasia was not observed (Fig. 4.J).

3.2. Immunohistochemical analysis

IL-17 and COX-2 immunoreactivities in the TC8 group were 21.9% and 11.9%, respectively in the glandular epithelium (Figs. 5.D and 6.D), whereas in the TC12 group, the IL-17 and COX-2 immunolabeling was

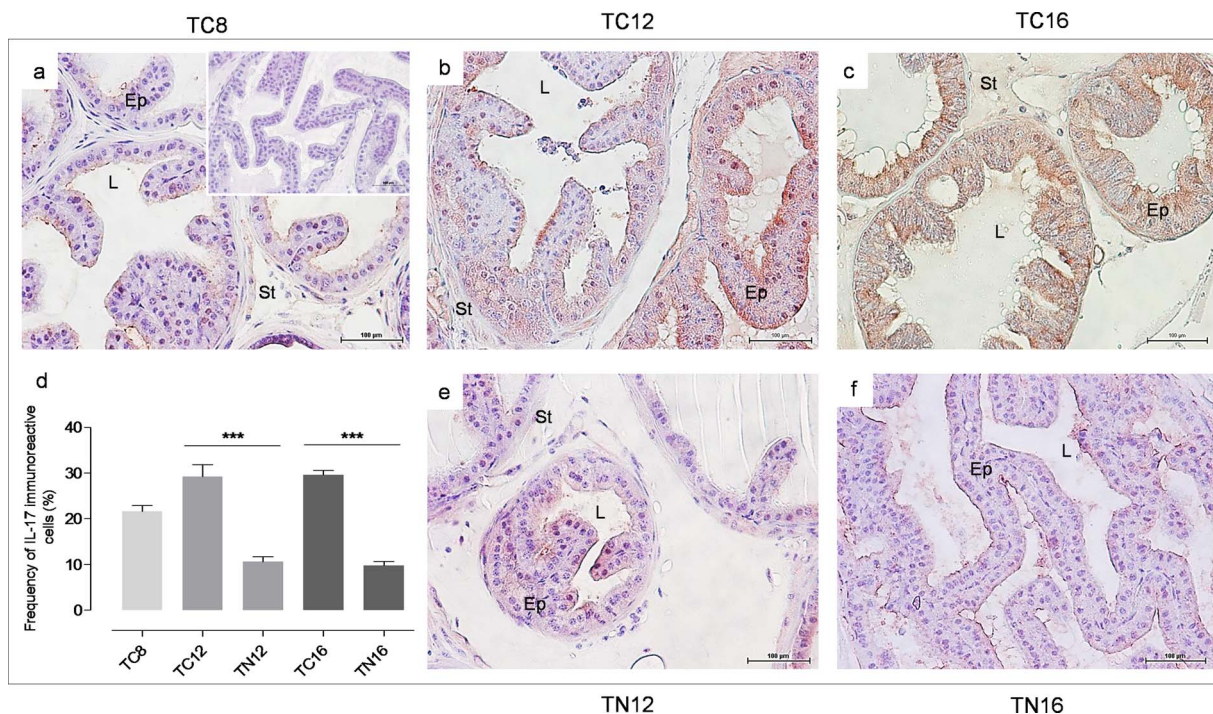


Fig. 5. Photomicrographs of IL-17 immunoreactivity A. TC8 group and negative control (inset) B. TC12 group C. TC16 group D. Frequency of IL-17 immunoreactive cells E. TN12 group F. TN16 group. * = $p < 0.05$, ** = $p < 0.01$, *** = $p < 0.001$.

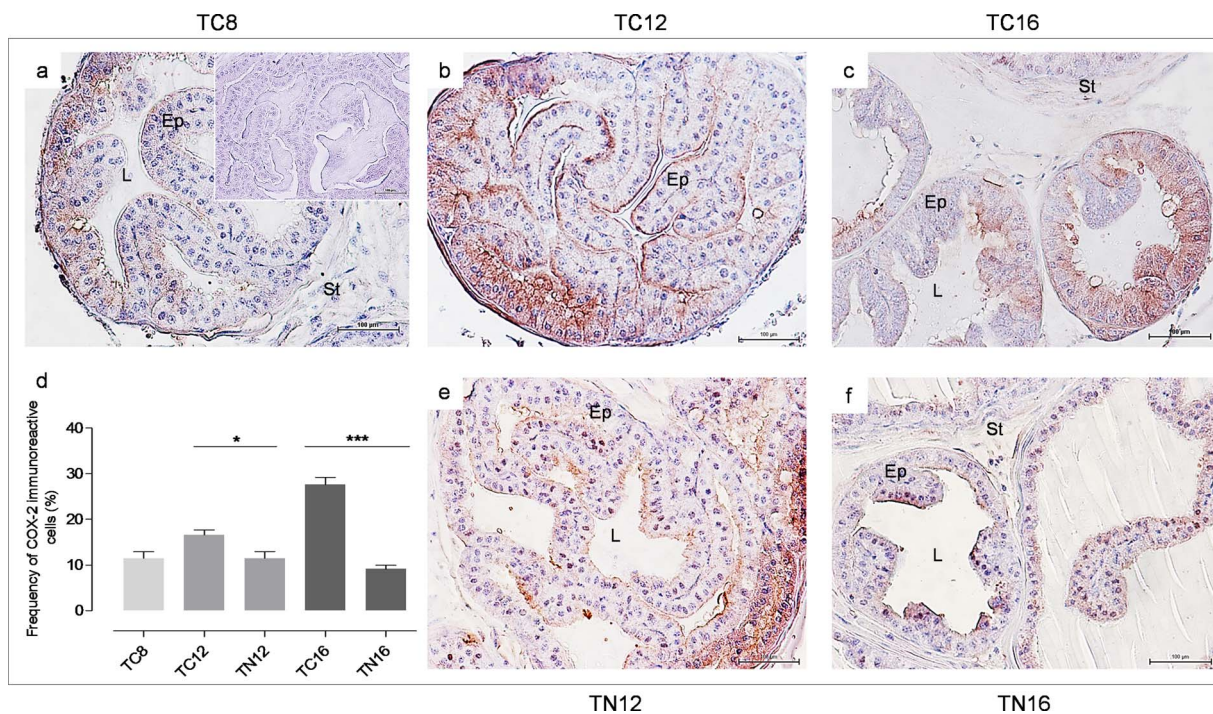


Fig. 6. Photomicrographs of COX-2 immunoreactivity A. TC8 group and negative control (inset) B. TC12 group C. TC16 group D. Frequency of COX-2 immunoreactive cells E. TN12 group F. TN16 group. * = $p < 0.05$, ** = $p < 0.01$, *** = $p < 0.001$.

28.1% and 16.3%, respectively (Figs. 5.D and 6.D).

In the TN12 group, there was a significant decrease in IL-17 and COX-2 immunoreactivities (Figs. 5.E and 6.E) in relation to the TC12 group, which represented 11.9% and 9.4%, respectively (Figs. 5.D and 6.D). The control group, euthanized at 16 weeks of age (TC16), showed increased immunoreactivity (Figs. 5.C and 6.C) when compared to the other control groups, with IL-17 immunoreactivity in the epithelium, representing 30% and 28.8% for COX-2 (Figs. 5.D and 6.D).

Finally, the treated group sacrificed at 16 weeks of age (TN16) also showed a significant decrease for inflammatory molecules (Figs. 5.F and 6.F), representing 10% for IL-17 immunoreactivity and 9.4% for COX-2 immunoreactivity in the glandular epithelium (Figs. 5.D and 6.D).

3.3. Western blotting analysis

The TC8 group showed a 30.2% level of COX-2 in relation to the β -

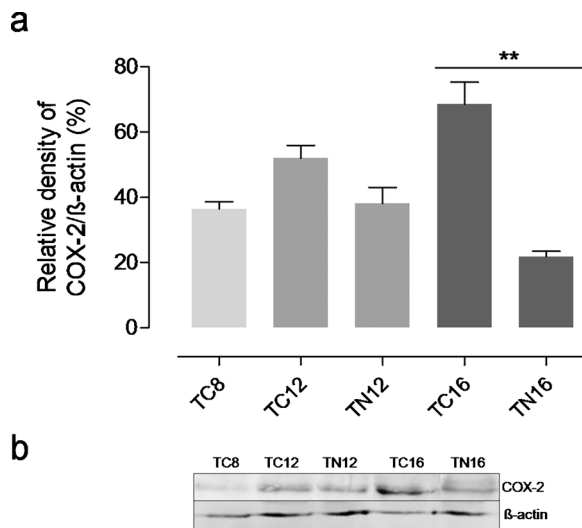


Fig. 7. A. Relative density of COX-2/β-actin (%). B. Western blotting bands. * = $p < 0.05$, ** = $p < 0.01$, *** = $p < 0.001$.

actin. The TC12 group presented a 51.5% COX-2 level, while TN12 showed 34.9%. TC16 and TN16 showed a significant difference between their COX-2 levels, representing 63.9 and 20.8%, respectively (Fig. 7.A and B).

4. Discussion

The results presented herein indicate that Nintedanib treatment was effective in delaying the progression of malignant lesions in the anterior lobe of the prostate of TRAMP mice. We observed that treated animals had a lower incidence of acinar epithelial tissue injuries compared to the control groups, particularly in the older mice. The results also indicate that the treatment is efficient in reducing important inflammatory biomarkers levels.

The TRAMP mice show progressive forms of prostatic cancer during disease development, including poorly differentiated and metastatic carcinomas, in addition to neuroendocrine characteristics (Berman-Booty et al., 2014). Usually, these mice show low grade PIN between 4 and 6 weeks of age. Between 6 and 10 weeks of age, there is an increase in the stratification of the epithelium leading to high grade PIN development. Between 10 and 16 weeks of age, the animals show high grade PIN with basement membrane disruption foci, characterizing well-differentiated carcinoma. In this age range, there is also hyperplastic and hypertrophic stromal development. Between the ages of 18 and 24 weeks, the mice present metastatic tumors (Gingrich et al., 1999). Since the FVB/NJ-TRAMP strain has a significantly higher incidence of malignant neuroendocrine carcinoma and a reduced lifetime, compared to the C57BL/6 strain, the disease in the former develops and progresses at a faster pace (Chiaverotti et al., 2008).

During prostatic oncogenesis progression, tumor cells with a high proliferative rate increase the demand on nutrients and oxygen. In addition, conditions as inflammatory infiltrate accumulation and fibrosis development decrease the efficiency of oxygen delivery, contributing to local hypoxia and secretion of pro-angiogenic factors, such as VEGF, that result in capillary formation from pre-existing blood vessels, increasing local vascularization (Hammam et al., 2013; Lee et al., 2009; Roberts et al., 2013). This process of new blood vessels formation, known as angiogenesis, is essential for the maintenance of chronic inflammation, as well as tumor growth and metastasis (Awasthi and Schwarz, 2015; Vasudev and Reynolds, 2014). Furthermore, it is known that in the long term, this vascularization contributes to the development of prostate reactive stroma (Montico et al., 2015) and the glandular microenvironment becomes favorable for the nutrition of

mutated cells and the progression of tumorigenesis (Dalglish and O'Byrne, 2006).

Angiogenesis, despite not being essential to the initial tumor development, it is essential for tumor growth, invasion and metastasis (Pratheeshkumar et al., 2012). VEGF is considered the main angiogenic modulator, and it is an important target for therapies involving angiogenesis delay. However, it is known that in its absence, other pathways such as FGF and PDGF can be activated, resulting in new blood vessel development (Fons et al., 2015). Therapeutic strategies involving the inhibition of the pathways related to angiogenesis may be useful as a procedure for prostate tumorigenesis intervention. Nintedanib is a compound that acts in blocking VEGFR, PDGFR and FGFR pathways, besides acting in the proliferation inhibition of endothelial cells, pericytes and smooth muscle cells (Hilberg et al., 2008). A study by Steinemann and collaborators, using cancer stem cells, reaffirmed Nintedanib antiproliferative properties when used as a single therapeutic agent *in vitro*. Treatment with this drug resulted in a sustained reduction in the capacity of colony formation in both cisplatin-resistant and cisplatin-sensitive GCT cells, and induced classical apoptosis (Steinemann et al., 2016).

Nintedanib has also indicated as clinically feasible in terms of safety and efficacy for the treatment of various tumors such as ovarian, renal cell carcinoma and even prostate cancer (Awasthi et al., 2015). The latest research reinforces the drug's efficacy, corroborating the results obtained by the study herein, which showed a delay in tumor progression in the anterior lobe of the prostate in TRAMP mice treated with Nintedanib. Nintedanib therapeutic effects have already been evaluated in several cancer types and its administration is approved for idiopathic pulmonary fibrosis and non-small lung cancer (Awasthi and Schwarz, 2015; Caglevic et al., 2015; Dhillon, 2015; McCormack, 2015). Also, treatments with other antiangiogenic drugs have shown promising results. In this way, Montico et al. (2015) observed the recovery of senescence-associated stromal changes in FVB male mice treated with TNP-470.

It is known that the release of soluble mediators such as cytokines, chemokines and reactive oxygen species (ROS) by macrophages and mast cells induced leucocyte mobilization and infiltration in the affected area, characterizing inflammation (Vendramini-Costa and Carvalho, 2012; De Visser et al., 2006). When the above response was maintained for a short period, there were therapeutic effects; however, when it became chronic, there was a great possibility of carcinogenesis development (Aggarwal et al., 2006; Medzhitov, 2010). The pro-inflammatory cytokines, secreted by immune cells, activate tumor-associated pathways involved in the proliferation, migration and invasion of tumor cells toward the stroma (Shigdar et al., 2014). Pro-inflammatory cytokines concentration increase, such as Interleukin-17 (IL-17), was associated with aging and also with prostate cancer development (De Angulo et al., 2015). In addition, IL-17 is a cytokine produced and secreted primarily by Th17 cells, playing opposite roles in tumor development: the IL-17 cytotoxic response towards the tumor cells might result in tumor regression; on the other hand, its secretion can also cooperate with tumor progression by inducing the release of pro-inflammatory cytokines and neutrophils mobilizers chemokines (Maniati et al., 2010; Murugaiyan and Saha, 2009). Nowadays, studies revealed the association between IL-17 expression and some angiogenesis promoting factors such as VEGF, specifically by activating STAT3/GIV signaling (Pan et al., 2015; Wu et al., 2016; Yang et al., 2014). The IL-17 results obtained in the present study are in agreement with other studies, considering the role of cytokines in angiogenesis and tumor progression.

Nintedanib treatment reduced significantly IL-17 immunoreactivity in the anterior lobe of the prostate. The major difference was observed between control and treated groups with 16 week old mice, indicating that this treatment played an effective role in delaying the inflammatory process during intermediary grades of carcinogenesis progression.

Another inflammatory biomarker evaluated in the present study was COX-2 which is an inducible enzyme, found in low concentrations, except in cases of tissue trauma and several types of cancer, when its expression is induced (Kido et al., 2016; Kulkarni et al., 2001; Liu and Rose, 1996; Tsujii et al., 1997). COX-2 gene is overexpressed in the presence of cytokines, growth factors and tumor stimulant factors, indicating its relation to inflammatory processes and making this enzyme an important target to identify inflammatory sites and cancer (Kummer and Coelho, 2002; Uddin et al., 2011). In the present study, COX-2 immunoreactivity was significantly diminished by Nintedanib treatment, particularly in the older mouse group. These results were in agreement to those found for IL-17.

Also, it is known that COX-2 expression is related to angiogenic factors production and carcinogenic potential of cells (Vendramini-Costa and Carvalho, 2012; Hamid et al., 2011). During the inflammation-induced angiogenesis, inflammatory cells are recruited, increasing the damage to the tissue and creating a pro-carcinogenic environment (Kim et al., 2013). The results obtained herein reinforced the close relation between the angiogenic and inflammatory processes, since the administration of Nintedanib, an antiangiogenic drug, resulted in decrease in inflammation biomarkers.

Finally, the results obtained by the present study showed Nintedanib treatment efficacy in decreasing the levels of COX-2 and IL-17 significantly in both ages analyzed. These results indicate that even though Nintedanib is not directly related to inflammation, it may adversely affect inflammatory pathways, leading to a delay in tumor progression. Further clinical tests are desirable for validation of the Nintedanib effects observed by the present study, since the animal model used (transgenic mice) could be considered limited due the complexity of the genesis, physiology, and progress of human malignancies (Mak et al., 2014).

5. Conclusion

The results presented herein showed that Nintedanib treatment led to a tumorigenesis delay in the anterior prostate lobe of the TRAMP model in early and intermediate grades of cancer development. Nintedanib administration resulted not only in decreased tumor lesions development but also in decreased inflammatory factors levels, reinforcing the close association between oncogenic and inflammatory pathways. Thus, Nintedanib is a promising drug against prostate cancer, considering the association of different signaling pathways.

Conflict of interest

The authors declare that there is not conflict of interest.

Ethical approval

All applicable international, national, and/or institutional guidelines for the care and use of animals were followed. (Committee for Ethics in Animal Research – University of Campinas, protocol n°: 4020-1)

Acknowledgement

This work was supported by São Paulo Research Foundation FAPESP (2015/16747-3)-Brazil.

References

Aggarwal, B., Shishodia, S., Sandur, S., Pandey, M., Sethi, G., 2006. Inflammation and cancer: how hot is the link? *Biochem. Pharmacol.* 72, 1605–1621. <http://dx.doi.org/10.1016/j.bcp.2006.06.029>.

Awasthi, N., Schwarz, R., 2015. Profile of nintedanib in the treatment of solid tumors: the evidence to date. *Oncotargets Ther.* 8, 3691–3701. <http://dx.doi.org/10.2147/OTT.S78805>.

Awasthi, N., Hinz, S., Brekken, R., Schwarz, M., Schwarz, R., 2015. Nintedanib, a triple angiokinase inhibitor, enhances cytotoxic therapy response in pancreatic cancer. *Cancer Lett.* 358, 59–66. <http://dx.doi.org/10.1016/j.canlet.2014.12.027>.

Barron, D., Rowley, D., 2012. The reactive stroma microenvironment and prostate cancer progression. *Endocr. Relat. Cancer* 19, R187–R204. <http://dx.doi.org/10.1530/ERC-12-0085>.

Berman-Booty, L.D., Sargeant, A.M., Rosol, T.J., Rengel, R.C., Clinton, S.K., Chen, C.-S., Kulp, S.K., 2012. A review of the existing grading schemes and a proposal for a modified grading scheme for prostatic lesions in TRAMP mice. *Toxicol. Pathol.* 40, 5–17. <http://dx.doi.org/10.1177/0192623311425062>.

Berman-Booty, L., Thomas-Ahner, J., Bolon, B., Oglesbee, M., Clinton, S., Kulp, S., Chen, C.-S., Perle, K., 2014. Extra-prostatic transgene-associated neoplastic lesions in transgenic adenocarcinoma of the mouse prostate (TRAMP) mice. *Toxicol. Pathol.* 43, 186–197. <http://dx.doi.org/10.1177/0192623314531351>.

Bousquet, G., Alexandre, J., Le Tourneau, C., Goldwasser, F., Faivre, S., Mont-Serrat, H., Kaiser, R., Misset, J., Raymond, E., 2011. Phase I study of BIBF 1120 with docetaxel and prednisone in metastatic chemo-naïve hormone-refractory prostate cancer patients. *Br. J. Cancer* 105, 1640–1645. <http://dx.doi.org/10.1038/bjc.2011.440>.

Čaglević, C., Grassi, M., Racz, L., Listi, A., Giallombardo, M., Bustamante, E., Gil-Bazo, I., Rolfo, C., 2015. Nintedanib in non-small cell lung cancer: from preclinical to approval. *Ther. Adv. Respir. Dis.* 9, 164–172. <http://dx.doi.org/10.1177/1753465815579608>.

Chiaverotti, T., Couto, S., Donjacour, A., Mao, J.-H., Nagase, H., Cardiff, R., Cunha, G., Balmain, A., 2008. Dissociation of epithelial and neuroendocrine carcinoma lineages in the transgenic adenocarcinoma of mouse prostate model of prostate cancer. *Am. J. Pathol.* 172, 236–246. <http://dx.doi.org/10.2353/ajpath.2008.070602>.

Dalgleish, A., O'Byrne, K., 2006. Inflammation and cancer: the role of the immune response and angiogenesis. *Cancer Treat. Res.* 130, 1–38. <http://dx.doi.org/10.1007/978-2-26283-0-1>.

De Angulo, A., Faria, R., Daniel, B., Jolly, C., DeGraffenried, L., 2015. Age-related increase in IL-17 activates pro-inflammatory signaling in prostate cells. *Prostate* 75, 449–462. <http://dx.doi.org/10.1002/pros.22931>.

De Marzo, A., Meeker, A., Zha, S., Luo, J., Nakayama, M., Platz, E., Isaacs, W., Nelson, W., 2003. Human prostate cancer precursors and pathobiology. *Urology* 62, 55–62. <http://dx.doi.org/10.1016/j.urolgy.2003.09.053>.

De Visser, K., Eichten, A., Coussens, L., 2006. Paradoxical roles of the immune system during cancer development. *Nat. Rev. Cancer* 6, 24–37. <http://dx.doi.org/10.1038/nrc1782>.

Dhillon, S., 2015. Nintedanib: a review of its use as second-line treatment in adults with advanced non-small cell lung cancer of adenocarcinoma histology. *Target. Oncol.* 10, 303–310. <http://dx.doi.org/10.1007/s11523-015-0367-8>.

Fons, P., Gueguen-Dorbes, G., Herault, J.-P., Geronimi, F., Tuyaret, J., Frédérique, D., Schaeffer, P., Volle-Challier, C., Herbert, J.-M., Bono, F., 2015. Tumor vasculature is regulated by FGF/FGFR signaling-mediated angiogenesis and bone marrow-derived cell recruitment: this mechanism is inhibited by SSR128129E, the first allosteric antagonist of FGFRs. *J. Cell. Physiol.* 230, 43–51. <http://dx.doi.org/10.1002/jcp.24656>.

Gingrich, J., Barrios, R., Foster, B., Greenberg, N., 1999. Pathologic progression of autochthonous prostate cancer in the TRAMP model. *Prostate Cancer Prostatic Dis.* 2, 70–75. <http://dx.doi.org/10.1038/sj.pcan.4500296>.

Hamid, A.R., Umbas, R., Mochtar, C.A., 2011. Recent role of inflammation in prostate diseases: chemoprevention development opportunity. *Acta Med. Indones.* 43, 59–65.

Hammam, O., Mahmoud, O., Zahran, M., Sayed, A., Salama, R., Hosny, K., Farghly, A., 2013. A possible role for TNF- α in coordinating inflammation and angiogenesis in chronic liver disease and hepatocellular carcinoma. *Gastrointest. Cancer Res.* 6, 107–114.

Hilberg, F., Roth, G., Krssak, M., Kautschitsch, S., Sommergruber, W., Tontsch-Grunt, U., Garin-Chesa, P., Bader, G., Zoepfel, A., Quant, J., Heckel, A., Rettig, W., 2008. BIBF 1120: triple angiokinase inhibitor with sustained receptor blockade and good anti-tumor efficacy. *Cancer Res.* 68, 4774–4782. <http://dx.doi.org/10.1158/0008-5472.CAN-07-6307>.

Kido, L.A., Montico, F., Sauce, R., Macedo, A.B., Minatel, E., Vendramini Costa, D.B., De Carvalho, J.E., Pilli, R.A., Cagnon, V.H.A., 2016. Anti-inflammatory therapies in TRAMP mice: delay in PCa progression. *Endocr. Relat. Cancer* 23, 235–250. <http://dx.doi.org/10.1530/ERC-15-0540>.

Kim, Y.-W., West, X.Z., Byzova, T.V., 2013. Inflammation and oxidative stress in angiogenesis and vascular disease. *J. Mol. Med. (Berl.)* 91, 323–328. <http://dx.doi.org/10.1007/s00109-013-1007-3>.

Kulkarni, S., Rader, J.S., Zhang, F., Liapis, H., Koki, A.T., Masferrer, J.L., Subbaramaiah, K., Dannenberg, A.J., 2001. Cyclooxygenase-2 is overexpressed in human cervical cancer. *Clin. Cancer Res.* 7, 429–434.

Kummer, C., Coelho, T., 2002. Cyclooxygenase-2 inhibitors nonsteroid anti-inflammatory drugs: current issues. *Rev. Bras. Anestesiol.* 52, 498–512. <http://dx.doi.org/10.1590/S0034-70942002000400014>.

Lee, H., Han, J., Bai, H.-J., Kim, K.-W., 2009. Brain angiogenesis in developmental and pathological processes: regulation, molecular and cellular communication at the neurovascular interface. *FEBS J.* 276, 4622–4635. <http://dx.doi.org/10.1111/j.1742-4658.2009.07174.x>.

Liu, X.H., Rose, D.P., 1996. Differential expression and regulation of cyclooxygenase-1 and -2 in two human breast cancer cell lines. *Cancer Res.* 56, 5125–5127.

Mak, I.W.Y., Evaniew, N., Gert, M., 2014. Lost in translation: animal models and clinical trials in cancer treatment. *Am. J. Transl. Res.* 1943-8141/AJTR1312010.

Maniati, E., Soper, R., Hagemann, T., 2010. Up for mischief? IL-17/Th17 in the tumour microenvironment. *Oncogene* 29, 5653–5662. <http://dx.doi.org/10.1038/onc.2010.367>.

McCormack, P.L., 2015. Nintedanib: First Global Approval. *Drugs* 75, 129–139. <http://dx.doi.org/10.1007/s11523-015-0367-8>.

- doi.org/10.1007/s40265-014-0335-0.
- Medzhitov, R., 2010. Inflammation 2010: new adventures of an old flame. *Cell* 140, 771–776. <http://dx.doi.org/10.1016/j.cell.2010.03.006>.
- Mimeault, M., Batra, S., 2013. Development of animal models underlining mechanistic connections between prostate inflammation and cancer. *World J. Clin. Oncol.* 4, 4–13. <http://dx.doi.org/10.5306/wjco.v4.i1.4>.
- Montico, F., Kido, L., San Martin, R., Rowley, D., Cagnon, V., 2015. Reactive stroma in the prostate during late life: the role of microvasculature and antiangiogenic therapy influences. *Prostate* 75, 1643–1661. <http://dx.doi.org/10.1002/pros.23045>.
- Murugaiyan, G., Saha, B., 2009. Protumor vs antitumor functions of IL-17. *J. Immunol.* 183, 4169–4175. <http://dx.doi.org/10.4049/jimmunol.0901017>.
- Pan, B., Shen, J., Cao, J., Zhou, Y., Shang, L., Jin, S., Cao, S., Che, D., Liu, F., Yu, Y., 2015. Interleukin-17 promotes angiogenesis by stimulating VEGF production of cancer cells via the STAT3/GIV signaling pathway in non-small-cell lung cancer. *Sci. Rep.* 5. <http://dx.doi.org/10.1038/srep16053>.
- Pratheeshkumar, P., Son, Y.-O., Budhrāja, A., Wang, X., Ding, S., Wang, L., Hitron, A., Lee, J.-C., Kim, D., Divya, S., Chen, G., Zhang, Z., Luo, J., Shi, X., 2012. Luteolin inhibits human prostate tumor growth by suppressing vascular endothelial growth factor receptor 2-mediated angiogenesis. *PLoS One* 7, e52279. <http://dx.doi.org/10.1371/journal.pone.0052279>.
- Roberts, E., Cossigny, D., Quan, G., 2013. The role of vascular endothelial growth factor in metastatic prostate cancer to the skeleton. *Prostate Cancer* 2013, 418340. <http://dx.doi.org/10.1155/2013/418340>.
- Sfanos, K., de Marzo, A., 2012. Prostate cancer and inflammation: the evidence. *Histopathology* 60, 199–215. <http://dx.doi.org/10.1111/j.1365-2559.2011.04033.x>.
- Shigdar, S., Li, Y., Bhattacharya, S., O'Connor, M., Pu, C., Lin, J., Wang, T., Xiang, D., Kong, L., Wei, M., Zhu, Y., Zhou, S., Duan, W., 2014. Inflammation and cancer stem cells. *Cancer Lett.* 345, 271–278. <http://dx.doi.org/10.1016/j.canlet.2013.07.031>.
- Siegel, R., Miller, K., Jemal, A., 2016. Cancer statistics, 2016. *CA Cancer J. Clin.* 66, 7–30. <http://dx.doi.org/10.3322/caac.21332>.
- da Silva, R.F., Nogueira-Pangrazi, E., Kido, L.A., Montico, F., Arana, S., Kumar, D., Raina, K., Agarwal, R., Cagnon, V.H.A., 2017. Nintedanib antiangiogenic inhibitor effectiveness in delaying adenocarcinoma progression in Transgenic Adenocarcinoma of the Mouse Prostate (TRAMP). *J. Biomed. Sci.* 24, 31. <http://dx.doi.org/10.1186/s12929-017-0334-z>.
- Steinemann, G., Jacobsen, C., Gerwing, M., Hauschild, J., Von Amsberg, G., Höpfner, M., Nitzsche, B., Honecker, F., 2016. Activity of nintedanib in germ cell tumors. *Anticancer Drugs* 27, 89–98. <http://dx.doi.org/10.1097/CAD.0000000000000305>.
- Tsujii, M., Kawano, S., DuBois, R.N., 1997. Cyclooxygenase-2 expression in human colon cancer cells increases metastatic potential. *Proc. Natl. Acad. Sci. U. S. A.* 94, 3336–3340.
- Tuxhorn, J., Ayala, G., Rowley, D., 2001. Reactive stroma in prostate cancer progression. *J. Urol.* 166, 2472–2483. [http://dx.doi.org/10.1016/S0022-5347\(05\)65620-0](http://dx.doi.org/10.1016/S0022-5347(05)65620-0).
- Uddin, M., Crews, B., Ghebreselasie, K., Huda, I., Kingsley, P., Ansari, M., Tantawy, M., Reese, J., Marnett, L., 2011. Fluorinated COX-2 inhibitors as agents in PET imaging of inflammation and cancer. *Cancer Prev. Res.* 4, 1536–1545. <http://dx.doi.org/10.1158/1940-6207>.
- Vasudev, N., Reynolds, A., 2014. Anti-angiogenic therapy for cancer: current progress, unresolved questions and future directions. *Angiogenesis* 17, 471–494. <http://dx.doi.org/10.1007/s10456-014-9420-y>.
- Vendramini-Costa, D., Carvalho, E., 2012. Molecular link mechanisms between inflammation and cancer. *Curr. Pharm. Des.* 18, 3831–3852. <http://dx.doi.org/10.2174/13816121280208370>.
- Weibel, E., 1963. Principles and methods for the morphometric study of the lung and other organs. *Lab. Investig.* 12, 131–155.
- Wollin, L., Maillat, I., Quesniaux, V., Holweg, A., Ryffel, B., 2014. Anti-fibrotic and anti-inflammatory activity of the tyrosine kinase inhibitor, nintedanib, in experimental models of lung fibrosis. *J. Pharmacol. Exp. Ther.* 349, 209–220. <http://dx.doi.org/10.1124/jpet.113.208223>.
- Wu, X., Yang, T., Liu, X., Guo, J., Nian, Xie, T., Ding, Y., Lin, M., Yang, H., 2016. IL-17 promotes tumor angiogenesis through Stat3 pathway mediated upregulation of VEGF in gastric cancer. *Tumor Biol.* 37, 5493–5501. <http://dx.doi.org/10.1007/s13277-015-4372-4>.
- Yang, B., Kang, H., Fung, A., Zhao, H., Wang, T., Ma, D., 2014. The role of interleukin 17 in tumour proliferation, angiogenesis, and metastasis. *Mediators Inflamm.* 2014 (2014), 623759. <http://dx.doi.org/10.1155/2014/623759>.
- Zynger, D., Yang, X., 2009. High-grade prostatic intraepithelial neoplasia of the prostate: the precursor lesion of prostate cancer. *Int. J. Clin. Exp. Pathol.* 2, 327–338.